Materials Today: Proceedings 33 (2020) 2474–2480

Contents lists available at ScienceDirect

Materials Today: Proceedings

journal homepage: www.elsevier.com/locate/matpr

Light scattering materials for energy-related applications: Determination of absorption and scattering coefficients

Junxin Wang [a], Annica M. Nilsson [a], David Barrios [b], William E. Vargas [c], Ewa Wäckelgård [a], Gunnar A. Niklasson [a,*]

[a] Department of Engineering Sciences, The Ångström Laboratory, Uppsala University, P.O.Box 534, SE-75121 Uppsala, Sweden
[b] Dept. Ingeniería Electrónica, Universidad Politécnica Salesiana, Guayaquil, Ecuador
[c] Centro de Investigación en Ciencia e Ingenieria de Materiales and Escuela de Física, Universidad de Costa Rica, 11501 San Jose, Costa Rica

ARTICLE INFO

Article history:
Available online 20 February 2020

Keywords:
Light scattering
Absorption coefficient
Scattering coefficient
Kubelka-Munk theory
Paint
Pigmented polymer
Suspended particle device

ABSTRACT

To facilitate optical design of energy-efficient materials and devices, a detailed knowledge of their basic optical parameters is necessary. In this paper we present a novel method for determining scattering (S) and absorption (K) coefficients from total transmittance and reflectance measurements by inversion of the Kubelka-Munk theory. The reflectance parameters appearing in this theory depend on the angular distribution of scattered light inside the material. The versatility of our method is demonstrated by a reanalysis of experimental data for several materials of interest in energy-related applications. Specifically, we report spectra of S and K for: (a) pigmented polymer foils for radiative cooling applications; (b) suspended particle devices for smart windows; (c) solar reflecting TiO_2-pigmented paints and (d) selective solar absorbing paints for solar collectors.

1. Introduction

Functional materials with applications in the fields of solar energy and energy-efficient buildings are frequently nano- or microstructured and exhibit significant light scattering. For example, it is possible to accurately tailor functional optical properties by incorporating absorbing and/or scattering particles in a non-absorbing solid matrix and varying particle concentration, size, shape and separation as well as layer thickness and surface roughness. Such materials have found wide application as pigmented paints [1], translucent sheets for daylighting applications [2], UV-absorbing films [3], radiative cooling devices [4,5], suspended particle devices [6,7] as well as solar absorbing paints for solar collectors [8,9]. An understanding of the optical properties of these materials is crucial in order to evaluate and optimize their performance.

In this paper, we focus on determining the effective optical parameters of composite materials consisting of particles in an embedding matrix. To facilitate optical design of such materials, a detailed knowledge of their basic optical parameters, namely the light scattering (S) and absorption (K) coefficients is necessary. Previous methods to extract these coefficients from experimental data either relied on unverified approximations [9] or required extensive computational effort. The two-background method [10] requires accurate characterization of white and black reference materials. The computationally complex approaches include Monte-Carlo simulations [11,12] and numerical solutions of the general radiative transfer equation [13,14]. A simpler alternative is offered by inversion schemes using the approximative two-flux theory [15,16]. However, it was found that in certain cases the obtained scattering and absorption coefficients could not accurately reproduce experimental spectra [7]. In this paper we present an improved method for inversion of the two-flux theory and demonstrate its versatility by calculations of S and K for various materials of interest for energy applications.

2. Inverse problem of Kubelka-Munk theory

The optical properties of a composite material depend on the type, size, shape and concentration of the particles together with the type of matrix. If the particle size is much smaller than the wavelength of light, effective medium theory [17,18] can be used to model the optical properties and light scattering can be

* Corresponding author.
E-mail address: gunnar.niklasson@angstrom.uu.se (G.A. Niklasson).

https://doi.org/10.1016/j.matpr.2020.01.339
2214-7853/

neglected. The effective optical constants of the composite layer can be obtained by inversion of experimental transmittance and reflectance measurements [19]. For particle sizes on the order of, or larger than the wavelength of light, light scattering becomes important and must be taken into account in optical theories. Scattering of light from a single spherical particle is described by Mie theory [20] and the case of multiple scattering in a composite material is usually treated within the framework of radiative transfer theory. The Kubelka-Munk two-flux model [21,22] is an analytical approximation to full radiative transfer, that is frequently used in applied research. It has been extended to the case of partly collimated and partly diffusely scattered light propagating in the material [15], and it constitutes a starting point for efforts to solve the inverse problem of radiative transfer for particulate composite materials. Below we give an overview of Kubelka-Munk theory and a recent improved formulation of the inverse problem, building on a previous paper by some of us [23]. It should be noted that the scattering coefficient S in the Kubelka-Munk model describes only the backscattering, as is clear from Eqs. (1) and (2) below.

A convenient approach to characterizing the optical properties of composite materials is to use a conventional spectrophotometer with an integrating sphere accessory. From spectrophotometric measurements, total transmittance (T_{tot}) and reflectance (R_{tot}), as well as the diffuse parts of the transmittance and reflectance (T_{dif}) and (R_{dif}) (Fig. 1a) are readily obtained. The regular transmittance (T_{reg}) and specular reflectance (R_{spe}) can subsequently be derived by subtracting the diffuse portions from the total ones [24]. The inverse problem of Kubelka-Munk theory consists in using experimentally measured total transmittance and reflectance in order to calculate the scattering and absorption coefficients of the material under study.

The Kubelka-Munk model [21,22] considers two radiation fluxes moving in the forward and backward direction in a slab of material (Fig. 1a). The total intensities in the forward and backward directions are coupled according to the differential equations:

$$\frac{dI}{dz} = -(S+K)I + SJ \tag{1}$$

$$\frac{dJ}{dz} = (S+K)J - SI \tag{2}$$

Here the intensity passing towards the back interface is denoted I and the intensity towards the front interface is denoted J. In addition $z = d\text{-}x$, and the coordinates $x = 0$ and d represent the back and front interfaces, respectively, in conformity with previously used notation [7,21–23]. The solutions of these equations give the transmittance and reflectance for the case of a slab with backside reflectance R_g (Fig. 1b), according to,

$$R_{KM} = \frac{1 - R_g[a - b\coth(bSd)]}{a - R_g + b\coth(bSd)} \tag{3}$$

and

$$T_{KM} = \frac{b(1-R_g)}{(a-R_g)\sinh(bSd) + b\cosh(bSd)} \tag{4}$$

where d is the thickness, a is equal to $(1 + K/S)$ and b is equal to $(a^2\text{-}1)^{0.5}$. After taking into account reflections at the front interface together with multiple reflections in the slab, we obtain

$$R = R_c + \frac{(1-R_c)(1-R_j)R_{KM}}{1 - R_j R_{KM}} \tag{5}$$

and

$$T = \frac{(1-R_c)T_{KM}}{1 - R_j R_{KM}} \tag{6}$$

where R_c is the reflectance of the incident light on the front interface of the slab while R_j is the frontside internal reflectance of the slab (Fig. 1b). It is realized, that in order to invert the equations for R and T to determine S and K, knowledge of the interface reflectance parameters is necessary. The internal interface reflectances R_g and R_j involve contributions from reflected collimated and diffuse light, at back and front interfaces, respectively (Fig. 1b),

$$R_{g,j} = (1 - q_{0,d})R_c + q_{0,d}R_{df,db}, \tag{7}$$

where q_0 and q_d are defined as the fractions of diffuse light in the film close to the back ($x = 0$) and front ($x = d$) interfaces, respectively. Furthermore, R_{df} and R_{db} are diffuse interface reflectances obtained from the forward and backward portions of the angle-dependent scattering profile [23]. Hence they describe diffuse reflection at the back and front interfaces, respectively. It has been shown by Barrios *et al* [7] that q_0 and q_d can be calculated from regular and diffuse transmittance together with specular and diffuse reflectance spectra. After some algebra, the relations for $q_{0,d}$ were found to be [7]

$$q_0 = \frac{T_{dif}(1-R_c)}{T_{tot}(1-R_c) - T_{reg}(R_{df} - R_c)} \tag{8}$$

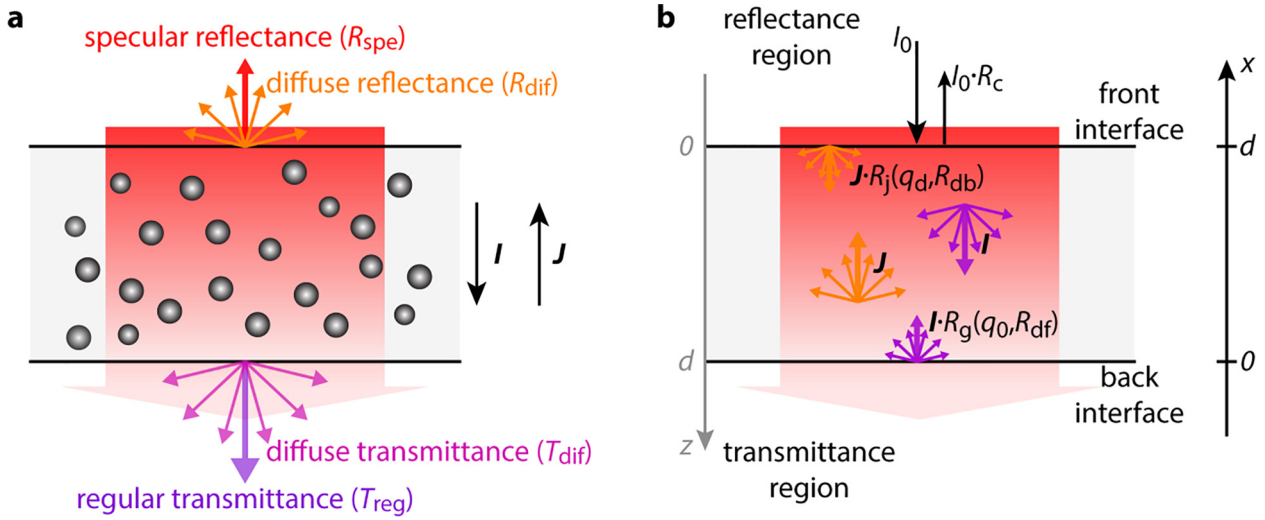

Fig. 1. (a) Schematic picture of transmittance and reflectance components, together with light propagation in two-flux model; (b) Illustration of parameters in the Kubelka-Munk two-flux model.

and

$$q_d = \frac{R_{dif}(1-R_c)}{R_{tot}(1-R_c) - R_{spe}(R_{db}-R_c) + R_c R_{db} - R_c} \quad (9)$$

It is seen from Eq. (7) that R_{df} and R_{db} need to be known in order to determine the total interface reflectances R_g and R_j. A problem here is that the diffusely scattered light exhibits a certain angular distribution and cannot in general be assumed to be isotropic. In recent works by some of us, we developed a method to estimate the diffuse interface reflectances of the composite medium by angle resolved scattering (ARS) measurements [23,25]. However, in many cases, for example in reanalysis of old data as in the present paper, ARS measurements may not be available. Hence, we have to assume an angular scattering profile in order to be able to determine the forward and backward diffuse interface reflectances R_{df} and R_{db}. We have investigated this problem extensively in the previous work [23] and found that strongly peaked forward and/or backward scattering distributions could be well approximated by a constant profile out to a cutoff angle given by the critical angle of total internal reflection. The alternative assumption would be isotropic diffuse scattering and combining these alternatives we proposed three approximations, denoted **dif**, **cri** and **cri/dif** [23].

In the **dif** approximation, we assumed an isotropic scattering profile for both forward and backward directions. We obtain the total diffuse interface reflectance with light incident from the sample to air from [26]

$$R_{df} = R_{db} = \frac{\int_{0^\circ}^{90^\circ} r(\beta)\sin(2\beta)d\beta}{\int_{0^\circ}^{90^\circ} \sin(2\beta)d\beta} \quad (10)$$

Here r denotes the reflectance for light incident on the interface from inside the composite material at an angle β.

In the **cri** approximation, we computed the diffuse interface reflectances in analogy with the **dif** method, but restricted the scattered light in the forward and backward directions to angles less than the critical angle, hence

$$R_{df} = R_{db} = \frac{\int_{0^\circ}^{\theta_c} r(\beta)\sin(2\beta)d\beta}{\int_{0^\circ}^{\theta_c} \sin(2\beta)d\beta} \quad (11)$$

The critical angle θ_c is the angle above which total internal reflection occurs so that the reflection coefficients for s- and p-polarized light are equal to unity. This angle exhibits a slight wavelength dependence, which has a negligible influence on the analysis. The critical angle was computed from the refractive indices of the matrix material and the air surrounding the composite slab.

In the **cri/dif** approximation, the scattering angle was assumed to be restricted by the critical angle in the forward direction and scattering was assumed to be isotropic in the backward direction.

$$R_{df} = \frac{\int_{0^\circ}^{\theta_c} r(\beta)\sin(2\beta)d\beta}{\int_{0^\circ}^{\theta_c} \sin(2\beta)d\beta} \quad (12)$$

$$R_{db} = \frac{\int_{0^\circ}^{90^\circ} r(\beta)\sin(2\beta)d\beta}{\int_{0^\circ}^{90^\circ} \sin(2\beta)d\beta} \quad (13)$$

3. Determination of absorption and scattering coefficients for energy-related materials

In this section we use the approach outlined above to calculate absorption and scattering coefficient spectra for several materials of interest pertaining to energy efficiency and solar energy. In some cases they constitute coatings deposited onto substrates. The substrates have refractive indices similar to those of the coatings and hence their effect on the optical parameters was ignored. We restrict ourselves to a reanalysis of selected data from the scientific literature. However, in certain cases considered below, only the total transmittance and reflectance were measured and little or no information was given on the diffuse and regular/specular parts. For weakly scattering materials, especially those having a low concentration of particles, it is usually a good approximation to put R_{spe} equal to the front surface reflectance, R_c, while independent information would be needed in order to approximate T_{reg} and T_{dif}. In the case of strongly scattering materials the situation is different and we may assume dominant diffuse scattering by putting $T_{dif} = T_{tot}$, and $R_{tot} = R_{dif} + R_c$. In the examples below the front surface reflectance was calculated from the refractive indices of the matrix materials embedding the particles.

3.1. Solar absorbing paints: FeMnCu oxide in KBr

High-efficiency solar-thermal energy conversion requires a coating with high solar absorptance and low thermal emittance of the solar collector [27]. Solar selective absorbing paints offer a commercially available low-cost alternative for applications in the low to medium temperature range [8]. These coatings consist of an absorbing pigment, usually iron oxide-based or carbon particles, in an organic resin. The coating is applied on a metallic solar collector surface. In this configuration, only reflectance is measurable, and the method in sect. 2 cannot be applied. Instead, it has been proposed [28,29] to use reflectance measurements on coatings with different thicknesses to obtain values of the Kubelka-Munk coefficients, S and K.

In order to study the optical properties of the efficiently solar absorbing FeMnCu oxide pigment, Tesfamichael et al. [9] dispersed the pigment particles in KBr. Details are given in the original publication [9]; briefly $(Fe,Mn)_3O_4$:CuO (Ferro Corporation, Model F-6331) was mixed with KBr powder, ground in a pearl mill and subsequently pressed into a pellet. The pellets had a diameter of 13 mm and a thickness (d) of 0.4 mm. Pigment particles were aggregated into clusters with a diameter of approximately 0.5 μm [9].

Fig. 2a shows the measured total transmittance and reflectance of a FeMnCu oxide-KBr sample with 0.1 wt% pigment, corresponding to a volume fraction of particles being 0.053%. The total reflectance is mainly caused by the interface reflectance from the front and back sample/air interfaces. The transmittance is lower in the visible than in the near infrared, implying a much higher absorption in the solar region than in the infrared. The diffuse parts of R and T were measured, but not reported in the original publication. However, it was possible to obtain the ratio between regular and total transmittance from the reported simplified evaluation of the S spectrum [9]. The specular reflectance was approximated by the front surface reflectance, which was obtained from the refractive index of KBr. This should be a good approximation for such an extremely low pigment volume fraction. The KBr matrix has a refractive index varying between 1.54 and 1.65 in the studied wavelength range [30], and for simplicity we put the critical angle equal to an average value of 39°. The spectra were analysed with the inversion method described in sect. 2, and it was found that both the **cri** and **cri/dif** approximations could be used to accurately fit both the reflectance and transmittance spectra in Fig. 2a. The obtained absorption and scattering coefficients are shown in Fig. 2b and clearly absorption is dominant. The fitted absorption coefficients from the two methods are almost overlapping, but the scattering coefficients exhibit large quantitative differences. Hence, it is critical for the evaluation of correct values of S and K, to use a good description of the angle-dependence of scattering. In the present case, we believe that the **cri** approximation is the

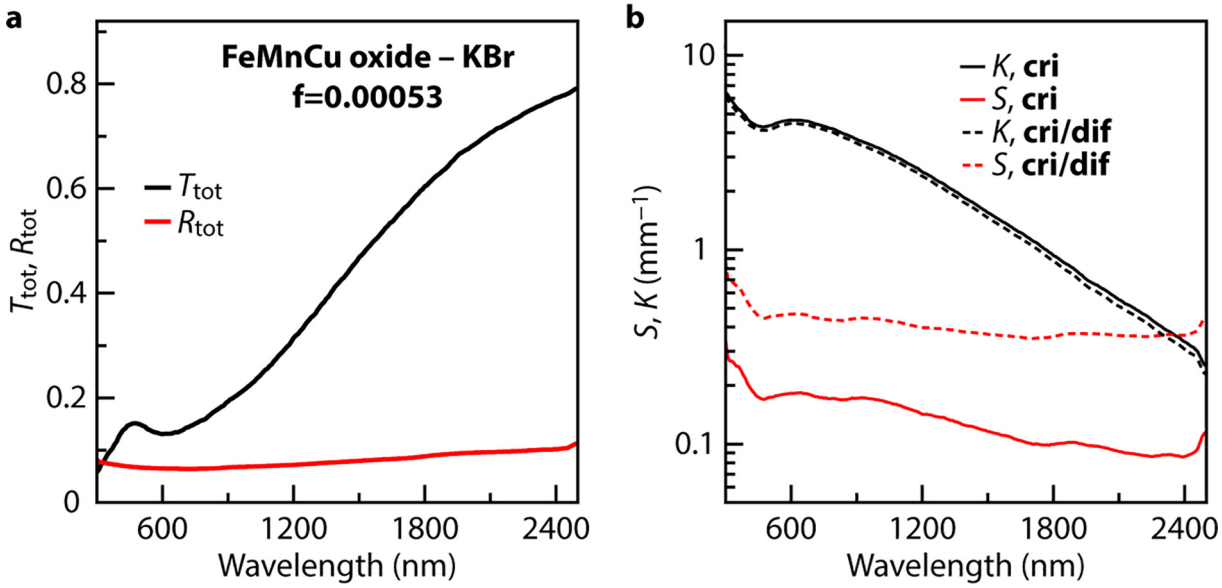

Fig. 2. (a) Total transmittance T_{tot} and total reflectance R_{tot} of a FeMnCu oxide-KBr sample with volume fraction of 0.00053 and thickness 0.4 mm; (b) Absorption coefficient K and scattering coefficient S derived using the **cri** and **cri/dif** approximations.

best one, in analogy with our previous studies [23] of low volume fraction nanoparticle composites.

3.2. Suspended particle devices

Suspended particle devices (SPDs) can rapidly switch from a dark bluish-black state to a clear grey appearance when a high AC electric field is applied [6,7]. Important applications of these devices occur in smart windows and in switchable optics technology. The optically active layer is made of a polymer matrix containing ~1 μm diameter droplets comprising a suspension of polyhalide particles [31]. This layer is sandwiched between glass substrates coated with transparent contacts. The SPD investigated in [6,7] has an active area of 28×22 cm^2 and a thickness of 300 μm. It was operated with a sinusoidal signal at 50 Hz and a peak voltage U between 0 (dark 'off' state) and 100 V (clear 'on' state).

In this case both the diffuse and regular/specular parts of the transmittance and reflectance were measured previously [7], so we could directly apply our improved inversion procedure to the data. Here the critical angle was estimated from the average refractive index of glass. Fig. 3a shows the spectra of T_{tot} and R_{tot} for both 'on' and 'off' states. The modulation on the transmittance curves between 'on' and 'off' states occurs mainly in the visible region. It was found that by using the **cri** approximation the computed total transmittance and reflectance curves overlap exactly with the experimental ones (Fig. 3a). This is a major improvement on the earlier analysis using the **dif** approximation [7], which could not accurately fit the reflectance spectrum. The absorption is dominant compared to the scattering (Fig. 3b), and it is mainly the absorption coefficient that is changed between the 'off' state and the 'on' state. It is observed that SPD devices fall into the category of low-scattering materials, which is of course a necessity for any application on windows.

3.3. Strongly scattering materials: TiO_2 particles in binder

Diffusely solar reflecting coatings can prevent excessive heating in strong sunlight and TiO_2 is an excellent choice of pigment for this application, due to its high refractive index. Below we report some results from an extensive previous study [32–34], in which the solar reflectance of coatings containing TiO_2 particles and TiO_2 coated SiO_2 particles was compared. Pure TiO_2 (rutile) pigment (Flexonyl White R 100 VP, Hoechst), with average particle diameter 230 nm, was mixed with a binder, a copolymer latex of ethylene vinyl acetate (Movolith, Hoechst). Paint coatings were deposited onto 2 mm thick glass plates by the doctor blading technique. Coatings with thickness between 60 and 75 μm, and particle weight fractions from 0.05 to 0.5, were obtained. Film thicknesses were measured over a step edge by a Tencor-Alpha-Step 200 surface profiler instrument. The refractive index of the binder was obtained from measurements on a coating of the pure binder. The average value in the studied wavelength range was found to be 1.36, giving a critical angle of 47°, while the critical angle of the glass substrate was approximately 41°. Fig. 4a depicts the transmittance and reflectance spectra for coatings with TiO_2 particle weight fractions of 0.05, 0.1, 0.2, 0.3, 0.4 and 0.5. The reflectance increases and the transmittance decreases as the pigment concentration increases. The abrupt drop in the near ultraviolet is due to the band gap of TiO_2, as well as to light absorption in the glass. The average solar reflectance of the high pigment concentration coatings is limited to about 0.8, but would of course be significantly higher when applied on a metal backing, for example on a roof.

The coatings were visually diffuse and preliminary ARS measurements did not show any specular peak in transmittance [35]. Hence it is a very good approximation to neglect the direct transmittance so that $T_{reg} = 0$ and in addition put $R_{spe} = R_c$. The Kubelka-Munk coefficients were extracted using the three approximations mentioned in section 2. However, the **cri** approximation failed to converge and is clearly not useful for such strongly scattering materials. The **cri/dif** approximation converges slightly better than the **dif** one, but both give qualitatively similar results. The obtained scattering and absorption coefficients S and K are depicted in Fig. 4b, clearly demonstrating that scattering is dominant in these paints. It seems that the scattering coefficient saturates when the weight fraction of TiO_2 reaches 0.4. Absorption bands in the near infrared range are due to the binder and the glass substrate.

3.4. Pigmented polymer foils for radiative cooling

Plastic foils containing non-absorbing pigments can display a high reflectance of solar radiation combined with a high transmit-

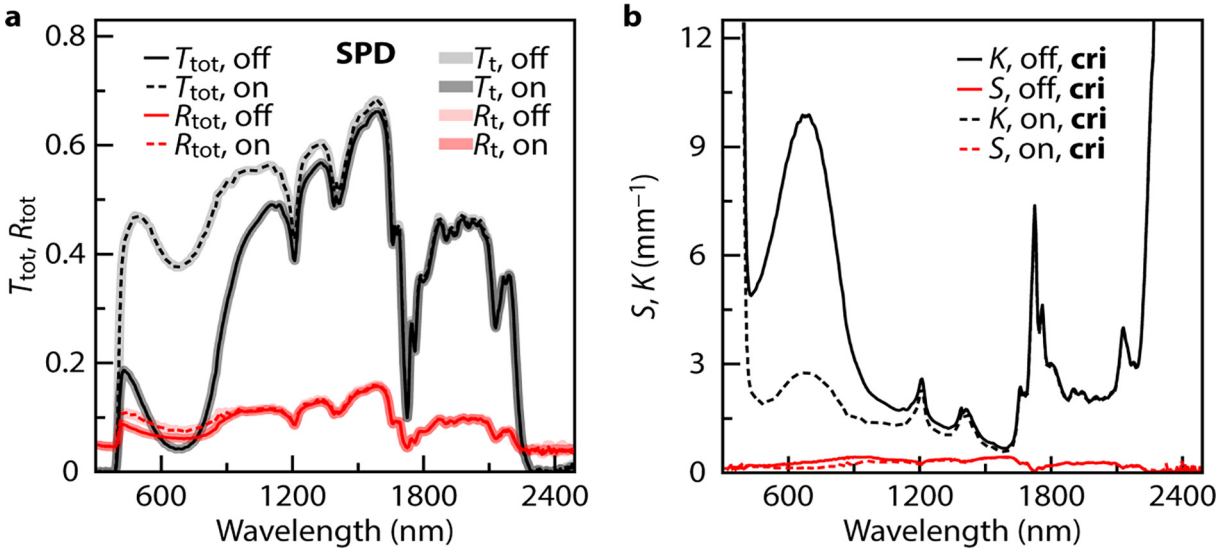

Fig. 3. (a) Experimental total transmittance T_{tot} and reflectance R_{tot}, and fitted (**cri**) total transmittance T_t and reflectance R_t when the SPD is in the 'on' and 'off' states; (b) K and S derived using the **cri** approximation for the 'on' and 'off' states. At wavelengths where the transmittance was close to zero, K could not be evaluated.

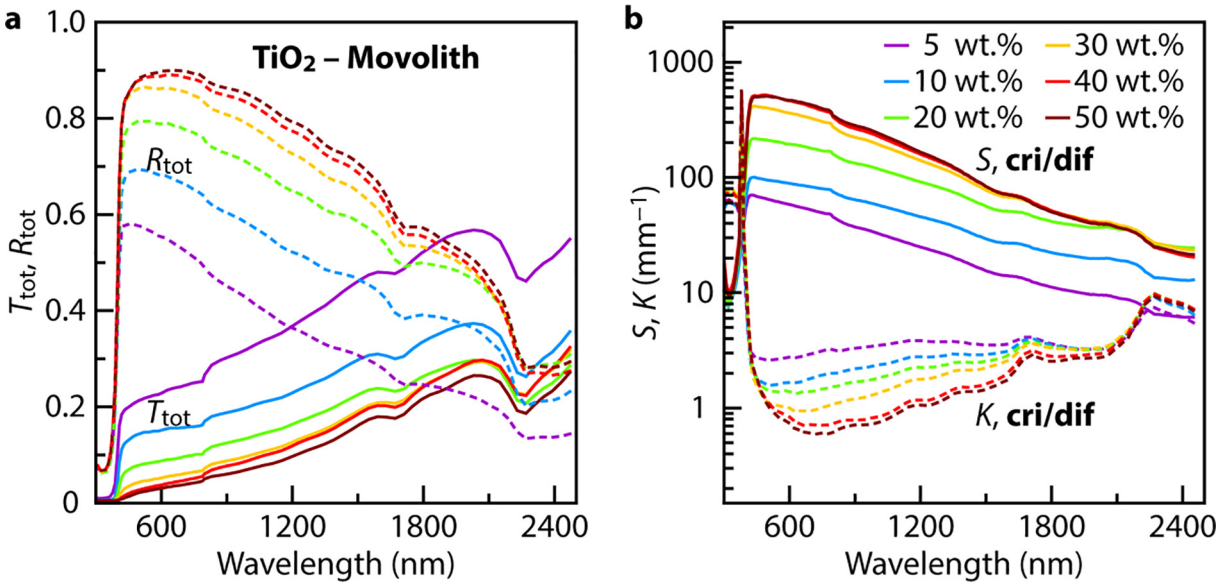

Fig. 4. (a) Total transmittance and reflectance spectra of TiO_2-Movolith samples with thicknesses of 63, 74, 63, 59, 62 and 71 μm for weight fractions of 0.05, 0.1, 0.2, 0.3, 0.4, and 0.5, respectively. (b) Scattering and absorption coefficients (S,K) computed from transmittance and reflectance data using the **cri/dif** approximation.

tance in the atmospheric window region in the thermal infrared [4]. They are suitable for keeping the temperature of an underlying thermally emissive material close to the ambient one. Heating by solar radiation is largely prevented and this is compensated, and can even be exceeded, by the infrared radiative cooling effect. Here we consider the optical scattering of ZnS-polyethylene radiative cooling foils [4]. We analyze data only in the visible and near infrared wavelength ranges, since scattering is very low in the thermal infrared. The pigment contained 98% ZnS particles with a mean diameter 0.15 μm, together with 1% $BaSO_4$, 0.2% ZnO and 0.8% unspecified materials. The powder was first heated to a temperature above 373 K to evaporate most of the water and was then mixed with polyethylene in an extruder during heating to 430 K in order to split pigment agglomerates. Subsequently, the mixture was pressed at a temperature of 420 K.

The total transmittance and reflectance spectra of ZnS-Polyethylene samples with two different volume fractions 0.0363 and 0.241 are depicted in Fig. 5a. The average solar reflectance is limited to 0.74 for the foil with the higher pigment volume fraction, due to absorption bands of unknown origin [4]. Hence the radiative cooling effect cannot wholly compensate solar heating. Scattering and absorption coefficients were obtained using our formulation of the inverse problem. The appearance of the samples was whitish diffuse and hence we neglect the regular transmittance as in sect. 3.3. Low density polyethylene has a refractive index of 1.48 to 1.52 in the considered spectral range [36], and for simplicity we use an average critical angle of 42°. The spectra of S and K are shown in Fig. 5b. Both the **cri/dif** and **dif** approximations converge and give very similar results. Also, in the case of these materials, scattering dominates over absorption.

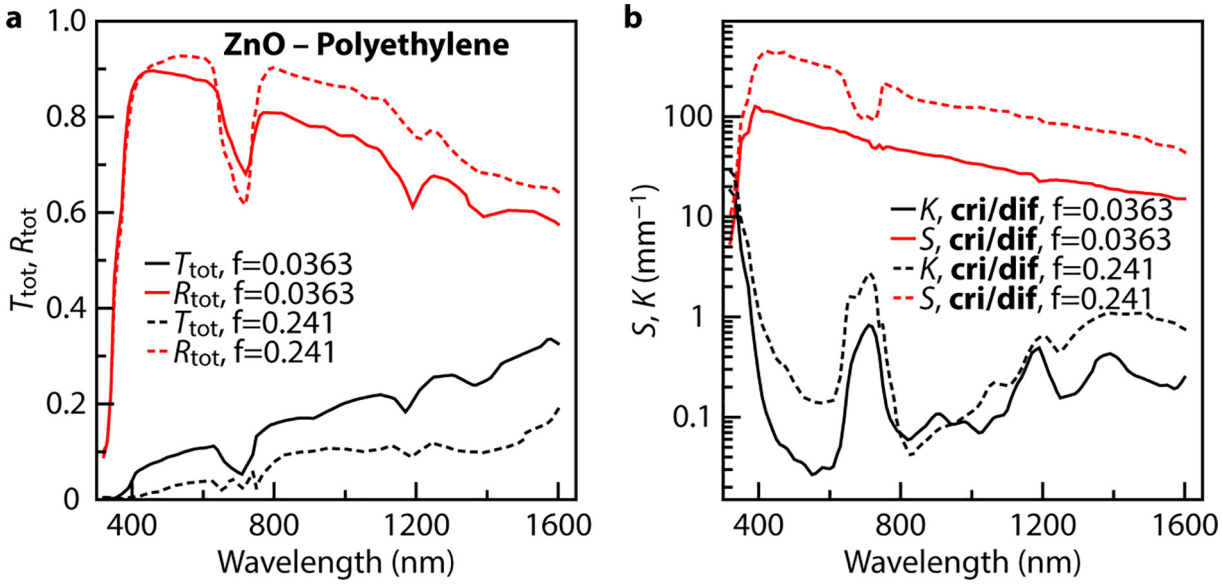

Fig. 5. (a) Total transmittance and reflectance spectra of ZnS-polyethylene samples with volume fraction of 0.0363 (d = 240 μm) and 0.241 (d = 140 μm); (b) Backscattering and absorption coefficients (S, K) computed from transmittance and reflectance data using the **cri/dif** approximation.

4. Conclusion

It is essential to develop reliable and robust methods to analyze the optical parameters of light scattering materials. In this paper, we analyzed weakly and strongly light scattering samples of interest for energy-related applications. The inverse problem of the two-flux Kubelka-Munk theory was solved in order to obtain reliable values of absorption and scattering coefficients. The main difficulty with this method is that experimental data that would be used to estimate the interface reflectances of the scattering layer are often lacking. We tested three approximations, denoted **cri**, **cri/dif**, and **dif** for the angular scattering profiles inside the material. It was found that the **cri** approximation is the most accurate one for weakly scattering samples. For strongly scattering samples both **cri/dif** and **dif** approximations can be used and give reasonable results. However, we hypothesize that **cri/dif** is most suitable for medium to strong scattering, and that for extremely strongly scattering samples **dif** should be used. It should be emphasized that all these methods are based on approximations to the angular light scattering profiles. In order to obtain very accurate results, actual measurements of angle resolved scattering are necessary.

Acknowledgements

This work was supported by the Swedish Research Council grant 2016-03713. We thank Cricursa S. A. for supplying SPD devices and Peter Greenwood for supplying the TiO_2 paints. We also acknowledge Tuquabo Tesfamichael and Torbjörn Nilsson for part of the reanalyzed experimental data.

References

[1] H.M. Shafey, Y. Tsuboi, M. Fujita, T. Makino, T. Kunitomo, Experimental study on spectral reflective properties of a painted layer, AIAA J. 20 (1982) 1747–1753.
[2] J.C. Jonsson, G.B. Smith, C. Deller, A. Roos, Directional and angle-resolved optical scattering of high-performance translucent polymer sheets for energy-efficient lighting and skylights, Appl. Opt. 44 (2005) 2745–2753.
[3] D. Koziej, F. Fischer, N. Kränzlin, W.R. Caseri, M. Niederberger, Nonaqueous TiO_2 nanoparticle synthesis: a versatile basis for the fabrication of self-supporting, transparent, and UV-absorbing composite films, ACS Appl. Mater. Interfaces 1 (2009) 1097–1104.
[4] T.M.J. Nilsson, G.A. Niklasson, C.G. Granqvist, A solar reflecting material for radiative cooling applications: ZnS pigmented polyethylene, Sol. Energy Mater. Sol. Cells 28 (1992) 175–193.
[5] Y. Zhai, Y. Ma, S.N. David, D. Zhao, R. Lou, G. Tan, R. Yang, X. Yin, Scalable-manufactured randomized glass-polymer hybrid metamaterial for daytime radiative cooling, Science 355 (2017) 1062–1066.
[6] D. Barrios, R. Vergaz, J.M. Sánchez-Pena, B. García-Cámara, C.G. Granqvist, G.A. Niklasson, Simulation of the thickness dependence of the optical properties of suspended particle devices, Sol. Energy Mater. Sol. Cells 143 (2015) 613–622.
[7] D. Barrios, R. Vergaz, J.M. Sanchez-Pena, C.G. Granqvist, G.A. Niklasson, Toward a quantitative model for suspended particle devices: Optical scattering and absorption coefficients, Sol. Energy Mater. Sol. Cells 111 (2013) 115–122.
[8] Z. Crnjak Orel, M. Klanjsek Gunde, A. Lencek, N. Benz, The preparation and testing of spectrally selective paints on different substrates for solar absorbers, Solar Energy 69 (Suppl. 6) (2001) 131–135.
[9] T. Tesfamichael, A. Hoel, G.A. Niklasson, E. Wäckelgård, M. Klanjsek Gunde, Z. Crnjak Orel, Optical characterization method for black pigments applied to solar-selective absorbing paints, Appl. Opt. 40 (2001) 1672–1681.
[10] E.M. Patterson, C.E. Shelden, B.H. Stockton, Kubelka-Munk optical properties of a barium sulfate white reflectance standard, Appl. Opt. 16 (1977) 729–732.
[11] Z.H. Levine, R.H. Streater, A.-M.R. Lieberson, A.L. Pintar, C.C. Cooksey, P. Lemaillet, Algorithm for rapid determination of optical scattering parameters, Opt. Express 25 (2017) 26728–26746.
[12] X. Liang, M. Li, J.Q. Lu, C. Huang, Y. Feng, Y. Sa, J. Ding, X.-H. Hu, Spectrophotometric determination of turbid optical parameters without using an integrating sphere, Appl. Opt. 55 (2016) 2079–2085.
[13] M.L. Meretska, R. Uppu, G. Vissenberg, A. Lagendijk, W.L. Ijzerman, W.L. Vos, Analytical modeling of light transport in scattering materials with strong absorption, Opt. Express 25 (2017) A906–A921.
[14] S. Leyre, F.B. Leloup, J. Audenaert, G. Durinck, J. Hofkens, G. Deconinck, P. Hanselaer, Determination of the bulk scattering parameters of diffusing materials, Appl. Opt. 52 (2013) 4083–4090.
[15] R. Levinson, P. Berdahl, H. Akbari, Solar spectral optical properties of pigments—Part I: model for deriving scattering and absorption coefficients from transmittance and reflectance measurements, Sol. Energy Mater. Sol. Cells 89 (2005) 319–349.
[16] R. Levinson, P. Berdahl, H. Akbari, Solar spectral optical properties of pigments—Part II: survey of common colorants, Sol. Energy Mater. Sol. Cells 89 (2005) 351–389.
[17] D.E. Aspnes, Local-field effects and effective-medium theory: A microscopic perspective, Am. J. Phys. 50 (1982) 704–709.
[18] G.A. Niklasson, C.G. Granqvist, O. Hunderi, Effective medium models for the optical properties of inhomogeneous materials, Appl. Opt. 20 (1981) 26–30.
[19] R.M.A. Azzam, N.M. Bashara, Ellipsometry and polarized light, North-Holland, New York, 1977.
[20] G. Mie, Beiträge zur Optik trüber Medien, speziell kolloidaler Metallösungen. Annalen der Physik 330 (1908) 377-445.
[21] P. Kubelka, F. Munk, Ein Beitrag zur Optik der Farbanstriche. Z Tech Phys. 12 (1931) 593-601.
[22] P. Kubelka, New Contributions to the optics of intensely light-scattering materials, Part I. J. Opt. Soc. Am. 38 (1948) 448–457.
[23] J. Wang, C. Xu, A.M. Nilsson, D.L.A. Fernandes, M. Strömberg, J. Wang, G.A. Niklasson, General method for determining light scattering and absorption of nanoparticle composites, Adv. Opt. Mater. (2018) 1801315.

[24] D. Rönnow, A. Roos, Correction factors for reflectance and transmittance measurements of scattering samples in focusing Coblentz spheres and integrating spheres, Rev. Sci. Instrum. 66 (1995) 2411–2422.
[25] J. Wang, C. Xu, A.M. Nilsson, D.L.A. Fernandes, G.A. Niklasson, A novel phase function describing light scattering of layers containing colloidal nanospheres, Nanoscale 11 (2019) 7404–7413.
[26] D.B. Judd, Fresnel reflection of diffusely incident light, J. Res. Nat. Bur. Stand. 29 (1942) 329–332.
[27] E. Wäckelgård, G.A. Niklasson, C.G. Granqvist, Selectively solar-absorbing coatings, in: J. Gordon (Ed.), Solar Energy: The state of the art, Janes & James, London, 2001, pp. 109–144.
[28] Z. Crnjak Orel, M. Klanjsek Gunde, B. Orel, Application of the Kubelka-Munk theory for the determination of the optical properties of solar absorbing paints, Progr. Opt. Coatings 30 (1997) 59–66.
[29] M. Klanjsek Gunde, Z. Crnjak Orel, Absorption and scattering of light by pigment particles in solar-absorbing paints, Appl. Opt. 39 (2000) 622–628.
[30] https://refractiveindex.info/?shelf=main&book=KBr&page=Li, (accessed 20.08.19.).
[31] S. Chakrapani, S.M. Slovak, R.L. Saxe, B. Fanning, SPD films and light valves comprising same. US Patent 6416827, July 9, 2002.
[32] W.E. Vargas, P. Greenwood, J.E. Otterstedt, G.A. Niklasson, Light scattering in pigmented coatings: experiments and theory, Solar Energy 68 (2000) 553–561.
[33] Vargas, W.E, Light Scattering and Absorption in Pigmented Coatings. Ph.D. Thesis, Uppsala University (1997).
[34] P. Greenwood, B.S. Gevert, J.E. Otterstedt, G.A. Niklasson, W.E. Vargas, Novel nano-composite particles: Titania-coated silica cores, Pigm. Resin Technol. 39 (2010) 135–140.
[35] Nostell, P. Private communication.
[36] https://www.filmetrics.com/refractive-index-database/Polyethylene/PE-Polyethene, (accessed 20.08.19.).